Enhancing optical switching with coherent control

Sunil Sandhu,[1,a)] Michelle L. Povinelli,[2] and Shanhui Fan[1]
[1]*E.L. Ginzton Laboratory, Stanford University, Stanford, California 94305, USA*
[2]*Ming Hsieh Department of Electrical Engineering, University of Southern California, Los Angeles, California 90089, USA*

(Received 31 March 2010; accepted 19 May 2010; published online 9 June 2010)

We show that coherent control can enhance the peak pulse energy coupled into a photonic crystal (PC) resonator system. We then demonstrate two applications of this coherent control technique in a bistable PC device, namely, the reduction in input power required to switch between its bistable states and the use of phase switching to switch between its bistable states. © *2010 American Institute of Physics*. [doi:10.1063/1.3449572]

The advances of laser pulse-shaping technologies[1–5] have led to much progress in the field of coherent control of light-matter interaction.[6–8] Generally, for coherent control, the goal is to tailor the relative phase between the different spectral components of an incident electromagnetic pulse in order to drive the system toward a desired final state, while canceling out paths that lead to undesirable outcomes.[6–8] Although originally demonstrated for controlling chemical reactivity,[9] coherent control has broadened into other fields with recent experimental demonstrations of applications in quantum optical information storage,[10] two-photon transitions,[11] and the enhancement of optically induced resonant transitions.[12] In Ref. 12, it was demonstrated that the application of a shaped laser pulse in resonance with a two-level atomic transition resulted in the excited level population being enhanced by about 2.5 times at its peak, relative to that achievable with transform-limited pulses.

In this paper, we show that coherent control can be similarly applied to an optical resonator system in order to enhance the peak transient energy coupled into the resonator. In addition, we numerically demonstrate two applications of this coherent control scheme in a bistable photonic crystal (PC) configuration,[13–15] namely, the reduction in the input power required to switch between its bistable states, and the use of phase switching to switch between its bistable states. We note that such a bistable device has been very extensively explored experimentally.[16–20]

As a concrete example, we consider the system in Fig. 1(a) which consists of a waveguide side coupled to a single-mode cavity having a resonant frequency of ω_{res}. The waveguide-resonator coupling rate is γ and the resonator has mode amplitude a(t), normalized such that $|a(t)|^2$ gives the energy in the mode. The incoming [outgoing] wave amplitude in the waveguide is denoted by $S_{in}(t)$ [$S_{out}(t)$] with $|S_{in}(t)|^2$ [$|S_{out}(t)|^2$] giving the power in the waveguide mode. The system can be described by the following coupled mode theory (CMT) equation, which has been previously shown to accurately describe light propagation in PC resonator systems[13]

$$\frac{da(t)}{dt} = j\omega_{res}a(t) - \gamma a(t) + j\sqrt{\gamma}S_{in}(t). \tag{1}$$

From Eq. (1), the temporal modal amplitude in the resonator can be written as

$$a(t) = \sqrt{\gamma}\int_{-\infty}^{\infty} \frac{S_{in}(\omega)e^{j\omega(t-t_0)}}{(\omega-\omega_{res})-j\gamma}d\omega, \tag{2}$$

where t_0 is the location of the peak of $S_{in}(t)$ and $S_{in}(\omega)$ is the Fourier transform of $S_{in}(t)$. As is evident in Eq. (2), the real part of the integrand's denominator undergoes a sign inversion about ω_{res}. This indicates that when the system is excited with a transform-limited input pulse $S_{in}(t)$, a destructive interference is induced between spectral components that are blueshifted and redshifted from ω_{res}, limiting the peak transient energy coupled into the resonator. Since the contribution of these off-resonant terms are highly sensitive to the spectral phase function of the input waveform $S_{in}(t)$, pulse-shaping techniques can be used to control the amount of pulse energy coupled into the resonator. In particular, the peak energy in the resonator $|a(t=t_0)|^2$ can be enhanced if the following phase function is applied to the spectral components $S_{in}(\omega)$ of the input pulse [Figs. 2(a) and 2(b)],

$$\varphi(\omega) = \arg[(\omega-\omega_{res})-j\gamma]. \tag{3}$$

In Fig. 2(c), we show the resulting temporal profile of the shaped input pulse, after the phase function in Eq. (3) is applied to a transform-limited pulse with a carrier frequency ω_0 located at a detuning of $\delta=(\omega_0-\omega_{res})/\gamma=2\sqrt{3}$ (the carrier frequency here is chosen for the bistable switching applica-

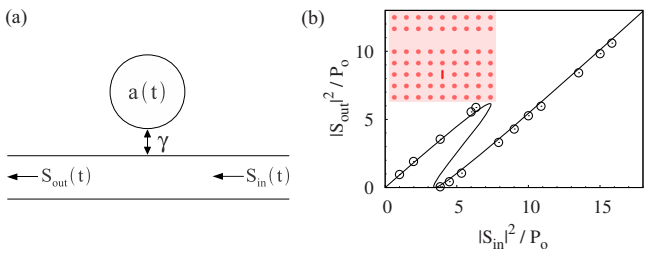

FIG. 1. (Color online) (a) Schematic of a coupled resonator-waveguide system. a(t) is the modal amplitude of the resonator, γ is its coupling rate to the waveguide, and $S_{in}(t)$ [$S_{out}(t)$] is the incoming [outgoing] wave in the waveguide. (b) Input vs output power plot obtained from CMT (solid line) and FDTD (open circles) for the coupled resonator-waveguide PC device shown in the inset.

a)Electronic mail: centaur@stanford.edu.

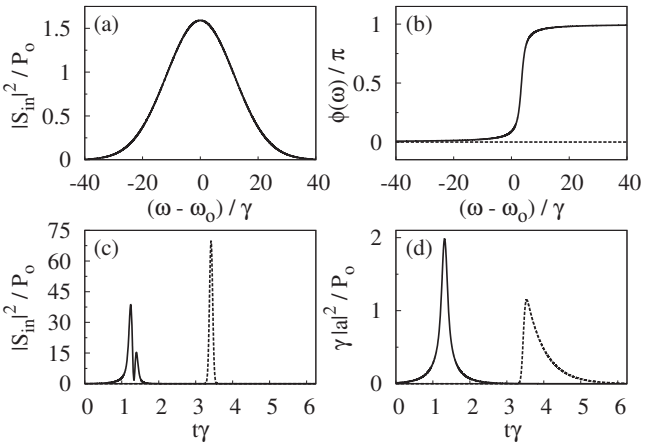

FIG. 2. (a) The power spectrum of an input pulse. (b) Phase spectra of the transform-limited pulse (dotted line) and a shaped pulse [Eq. (3)] (solid line). (c) Shaped pulse (solid line) and transform-limited pulse (dotted line) in the time domain, with power and phase spectra shown in Figs. 2(a) and 2(b), respectively. (d) Reflected power from the resonator [$|a(t)|^2$ is the energy coupled into the resonator].

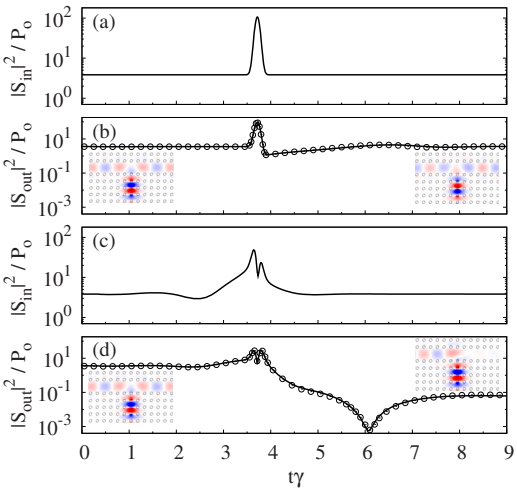

FIG. 3. (Color online) The (a) transform-limited input waveform and (c) shaped input waveforms used in the bistable switching analysis. (b) and (d) show transmitted powers corresponding to (a) and (c), respectively, from FDTD (solid line) and CMT (open circles) simulations. Insets in (b) and (d) show the electric field distributions before and after the application of the input pulse.

tion to be discussed below). Figure 2(d) shows the transient energy coupled into the resonator from the inputs in Fig. 2(c). We see in Fig. 2(d) that the shaped input pulse results in about 1.7 times enhancement in the peak transient energy coupled into the resonator as compared to the transform-limited input pulse.

As an application of the above coherent control technique, we now specialize to the bistable PC system shown in Fig. 1(b). The system consists of a square lattice of dielectric rods with refractive index n=3.5 and a radius of 0.2a (a=lattice constant) embedded in air (n=1). The waveguide in the PC is formed by removing a line of rods, and a side-coupled single mode resonator is formed by introducing a point defect in the form of an oval shaped dielectric rod, with major and minor axis lengths of 0.8a and 0.2a, respectively. The point defect region has a Kerr coefficient of $n_2=1.5\times10^{-17}$ m^2/W which is achievable in many nearly instantaneous nonlinear semiconductor materials.[21] The CMT equation of the system can be derived from Eq. (1) by adding the effect of Kerr nonlinearity in the resonator,[13]

$$\frac{da(t)}{dt} = j\left(\omega_{res} - \frac{\gamma^2|a(t)|^2}{P_0}\right)a(t) - \gamma a(t) + j\sqrt{\gamma}S_{in}(t), \qquad (4)$$

where P_0 is the characteristic power of the resonator.[15] The device in Fig. 1(b) has been previously shown to generate a high contrast between its bistable states in its transmission.[13] Here we show that by using coherent control, we can reduce the input threshold power required to switch between the two bistable states of the system, when a short input pulse is used for switching purposes.

We simulate the bistable behavior of the PC device using the nonlinear finite-difference time-domain (FDTD) method[22] for the TM case with electric field parallel to the rod axis. The simulations were performed at a resolution of 40×40 grid points per unit cell, with perfectly matched layer boundary conditions. The resonator is designed to have a resonant frequency of $\omega_{res}=0.3642(2\pi c/a)$ and the coupling between the waveguide and the resonator results in a quality factor of $\omega_{res}/2\gamma=4200$. The resonator has a characteristic power[15] of $P_0=6.74$ mW/μm for a wavelength of $\lambda_0=1.55$ μm. We start by using a continuous wave (cw) excitation, with the excitation's carrier frequency ω_0 located at a detuning of $\delta=2\sqrt{3}$ (where $\delta=\sqrt{3}$ is the minimum detuning requirement for the presence of bistability[15]). Figure 1(b) shows the system's transmitted power $|S_{out}(t)|^2$ versus input power $|S_{in}(t)|^2$, which exhibits a hysteresis behavior. We see that the system has a bistable region for $|S_{in}(t)|^2$ between $3.4P_0$ and $7.4P_0$.

We now consider the pulse dynamics of the system, and show that the input power required for bistable switching can be lowered when coherent control is used. To see the switching dynamics, the system is first excited to a power level $|S_{out}(t)|^2=3.6P_0$ in the upper hysteresis branch of Fig. 1(b) using a cw excitation with input power $|S_{in}(t)|^2=3.9P_0$. We then seek to switch the system to the lower branch in the hysteresis branch of Fig. 1(b), by applying an additional transient input pulse with the same carrier frequency detuning $\delta=2\sqrt{3}$ as the cw excitation. (The switching energy required is defined as the energy in such a transient input pulse.) The input power returned to the lower level $|S_{in}(t)|^2=3.9P_0$ after the transient pulse has passed through the system. To demonstrate the effect of coherent control we compare the switching action of the following two different pulses: the transform-limited input pulse [Fig. 3(a)] that has a full-width-half-maximum pulse width of 0.73 ps, and the shaped input pulse [Fig. 3(c)] that was prepared by applying the phase function in Eq. (3) to the spectra of the transform-limited pulse. We emphasize that these two pulses have the same power spectra and the same total pulse energy. Figures 3(b) and 3(d) show the transient power transmission that results from the inputs in Figs. 3(a) and 3(c), respectively. We see that whereas the shaped input pulse does result in the system switching to the lower hysteresis branch and, hence, a lower transmission after the switching pulsed has passed through the system [Fig. 3(d)], the transform-limited input pulse *with the same energy* is unable to switch the system [Fig. 3(b)]. The FDTD results agree very well with CMT calculations using Eq. (4). Our simulations show that with the same fixed spectral width of the input pulse, compared to a transform-limited pulse, the threshold input energy re-

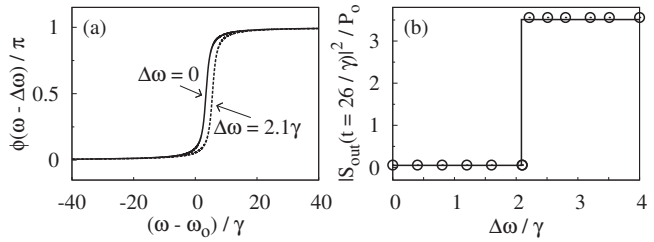

FIG. 4. (a) Phase functions for two different $\Delta\omega$ values. (b) Results from CMT (solid line) and FDTD (open circles) of the transmission output power $|S_{out}(t)|^2$ long after the switching pulse has passed, over a range of frequency detunings $\Delta\omega$ of the shaped pulse's phase function.

quired for switching the system is reduced by about 1.5 times when a shaped pulse is applied. This corresponds to a threshold input peak power reduction of about three times.

The use of coherent control also results in a novel phase switching capability in the bistable PC device. Since the peak energy coupled into the resonator is critically dependent on the phase spectrum of the input pulse, the switching action of the device should therefore be very sensitive on the phase. As an example, we consider a set of shaped input switching pulses, in which we apply a phase function $\varphi(\omega) = \arg[(\omega - \omega_0 - \Delta\omega) - j\gamma]$ for a range of $\Delta\omega$ values [Fig. 4(a)]. Figure 4(b) shows the transmitted output power of the system long after the switching pulse has passed. We see that by a very small variation in $\Delta\omega$ around the point 2.1γ, we can coherently control whether an input pulse will switch the system from the upper to lower hysteresis branch in Fig. 1(b).

To generate the pulse required for the phase switching, the input shaped pulse can be created using the "zero dispersion pulse compressor" and the programmable spatial light modulator (SLM) configuration, as discussed in Ref. 1. In this configuration, the frequency components of a transform-limited input pulse are first angularly dispersed by a grating, and then focused onto the SLM using a lens. After the phase modulation from the SLM, a second lens and grating recombine the output frequency components into a shaped pulse. The shift, $\Delta\omega$, in the frequency center at which phase modulation is applied can be directly programmed into the SLM.[1]

The simulations were performed at the Pittsburgh Supercomputing Center (PSC) and the National Center for Supercomputing Applications (NCSA). This work was supported by the Slow Light program at DARPA DSO, under AFOSR Grant No. FA9550-05-0414.

[1] A. M. Weiner, Rev. Sci. Instrum. **71**, 1929 (2000).
[2] G. Stobrawa, M. Hacker, T. Feurer, D. Zeidler, M. Motzkus, and F. Reichel, Appl. Phys. B: Lasers Opt. **72**, 627 (2001).
[3] A. Monmayrant and B. Chatel, Rev. Sci. Instrum. **75**, 2668 (2004).
[4] A. Präkelt, M. Wollenhaupt, A. Assion, and C. Horn, Rev. Sci. Instrum. **74**, 4950 (2003).
[5] Z. Jiang, C. B. Huang, D. E. Leaird, and A. M. Weiner, Nat. Photonics **1**, 463 (2007).
[6] W. S. Warren, H. Rabitz, and M. Dahleh, Science **259**, 1581 (1993).
[7] D. Goswami, Phys. Rep. **374**, 385 (2003).
[8] H. Rabitz, New J. Phys. **11**, 105030 (2009).
[9] M. Dantus and V. V. Lozovoy, Chem. Rev. (Washington, D.C.) **104**, 1813 (2004).
[10] N. S. Ginsberg, S. R. Garner, and L. V. Hau, Nature (London) **445**, 623 (2007).
[11] D. Meshulach and Y. Silberberg, Nature (London) **396**, 239 (1998).
[12] N. Dudovich, D. Oron, and Y. Silberberg, Phys. Rev. Lett. **88**, 123004 (2002).
[13] M. F. Yanik, S. Fan, and M. Soljacic, Appl. Phys. Lett. **83**, 2739 (2003).
[14] S. F. Mingaleev, A. E. Miroshnichenko, and Y. S. Kivshar, Opt. Express **15**, 12380 (2007).
[15] M. Soljačić, M. Ibanescu, S. G. Johnson, Y. Fink, and J. D. Joannopoulos, Phys. Rev. E **66**, 055601 (2002).
[16] E. Weidner, S. Combrié, A. d. Rossi, N.-V.-Q. Tran, and S. Cassette, Appl. Phys. Lett. **90**, 101118 (2007).
[17] M. Notomi, A. Shinya, S. Mitsugi, G. Kira, E. Kuramochi, and T. Tanabe, Opt. Express **13**, 2678 (2005).
[18] T. Tanabe, M. Notomi, S. Mitsugi, A. Shinya, and E. Kuramochi, Opt. Lett. **30**, 2575 (2005).
[19] P. E. Barclay, K. Srinivasan, and O. Painter, Opt. Express **13**, 801 (2005).
[20] X. Yang, C. Husko, C. W. Wong, M. Yu, and D.-L. Kwong, Appl. Phys. Lett. **91**, 051113 (2007).
[21] M. Sheik-Bahae, D. C. Hutchings, D. J. Hagan, and E. W. Van Stryland, IEEE J. Quantum Electron. **27**, 1296 (1991).
[22] A. Taflove and S. C. Hagness, *Computational Electrodynamics* (Artech House, Norwood, MA, 2000).